frontiers | Frontiers in Marine Science

TYPE Original Research
PUBLISHED 08 May 2025
DOI 10.3389/fmars.2025.1519668



OPEN ACCESS

EDITED BY
Baohong Chen,
Ministry of Natural Resources, China

REVIEWED BY
Daniel Rittschof,
Duke University, United States
Edgars Kuka,
Latvian State Institute of Wood Chemistry (LAS), Latvia

*CORRESPONDENCE
Licheng Peng
lcpeng@hainanu.edu.cn
Naiming Zhang
zhangnaiming@sina.com

RECEIVED 30 October 2024
ACCEPTED 15 April 2025
PUBLISHED 08 May 2025

CITATION
Gao L, Su Y, Mehmood T, Wang Z, Peng L and Zhang N (2025) UVA-induced weathering of microplastics in seawater: surface property transformations and kinetics.
*Front. Mar. Sci.* 12:1519668.
doi: 10.3389/fmars.2025.1519668



# UVA-induced weathering of microplastics in seawater: surface property transformations and kinetics

Liu Gao[1,2,3,4], Yuanyuan Su[2,3], Tariq Mehmood[5], Zezheng Wang[6], Licheng Peng[2,3]* and Naiming Zhang[1,4]*

[1]College of Resources and Environment, Yunnan Agricultural University, Kunming, China, [2]Key Laboratory of Agro-Forestry Environmental Processes and Ecological Regulation of Hainan Province, Hainan University, Haikou, China, [3]School of Environmental Science and Engineering, Hainan University, Haikou, China, [4]Yunnan Soil Fertility and Pollution Restoration Laboratory, Yunnan Agricultural University, Kunming, China, [5]Department Sensors and Modeling, Leibniz Institute for Agricultural Engineering and Bioeconomy (ATB), Potsdam, Germany, [6]State Key Laboratory of Freshwater Ecology and Biotechnology, Institute of Hydrobiology, Chinese Academy of Sciences, Wuhan, China

During environmental migration, large plastic fragments can undergo degradation into microplastics (MPs), posing a significant threat to ecosystems. A research gap exists in understanding how MPs age in complex environments. We modeled aging by integrating an aging index with degradation kinetics. This study investigated the degradation of MPs (polyethylene (PE), polypropylene (PP), polystyrene (PS) and polyvinyl chloride (PVC)) exposed to ultraviolet radiation in seawater. Aged MPs exhibited cracks, oxidized particles, and wrinkles on their surfaces. The functional groups experienced stretching (e.g., -OH, C-H, C=O) and bending (e.g., X-H in-plane, C-H in-plane), as identified through Fourier transform infrared spectroscopy (FTIR). Meanwhile, the crystallinity of MPs increased initially but decreased over time. The roughness and carbonyl index (CI) of MPs was increased as the weathering time progressed. mPE and mPP exhibited the most pronounced aging. The Elovich kinetic model poorly fitted the CI for aged MPs. A First-order kinetic improvement model fitted well but lacked clear parameter significance. The degradation mechanisms of mPE and mPP were similar. The benzene ring structure in mPS and dechlorination experienced by mPVC render them resistant to degradation. This study provides evidence that that enhances our understanding of the mechanisms underlying the aging process of MPs in seawater.

KEYWORDS

**aging time, carbonyl index, kinetics, microplastics, ultraviolet radiation**

# 1 Introduction

Plastic aging is a critical transformation process governing the environmental fate of plastic debris. During environmental migration, plastics undergo irreversible physicochemical alterations, including changes in surface roughness, hydrophobicity, crystallinity, and chemical bonding. These alterations are driven by exogenous forces such as solar radiation, wave action, and biological activity (Fu et al., 2019; Liu et al., 2020; Luo et al., 2020). These modifications profoundly influence plastics environmental interactions and ecotoxicological impacts. For instance, progressive fragmentation of plastic debris generates secondary microplastics (MPs) (Peng et al., 2020), while aging facilitates the leaching of additives (e.g., plasticizers and stabilizers) into surrounding ecosystems. Additives may interact synergistically with co-occurring pollutants like heavy metals and organic contaminants, forming complex pollutant matrices with amplified ecological risks (Fang et al., 2019; Ma et al., 2019).

The degree of MPs aging can be influenced by various factors, including polymer type, exposure time, temperature, moisture, salinity, and oxygen levels. Environmental stressors induce oxidative degradation and structural defects, enhancing porosity and creating reactive sites for ion adsorption on aged MPs (Brandon et al., 2016; Rochman et al., 2013; Stark and Matuana, 2004). MPs accelerated degradation has been observed under extreme conditions, such as elevated temperatures, Fenton reactions, or hydrogen peroxide treatments, which induce chain scission, cross-linking, and surface erosion (Ding et al., 2020; Dong et al., 2022; Lang et al., 2020). Among natural aging mechanisms, photocatalysis driven by ultraviolet (UV) radiation plays a dominant role (Sintim et al., 2019). Solar UVB (280–315 nm) and UVA (315–400 nm) irradiation generate free radicals on MPs surfaces, initiating oxidation, dehydrogenation, and backbone cleavage (Gewert et al., 2015). Notably, the types of polymers significantly modulate aging pathways: sulfuration promotes oxidation in micro-sized polyethylene (mPE), while micro-sized poly(butylene adipate-co-terephthalate) (mPBAT) undergoes reductive cleavage with concomitant organic compound release (Du et al., 2024). Distinct morphological changes have also been reported; micro-sized polypropylene (mPP) develops extensive surface cracks under UV exposure, whereas micro-sized polystyrene (mPS) exhibits minimal physical degradation (Cai et al., 2018). Hence, it is important to systematically investigate the structural characteristics of diverse MPs types under UV radiation. We hypothesized that different categories of MPs age differently.

Existing studies predominantly employ laboratory simulations to investigate MPs aging in controlled environments, including soil, beach sand, ultrapure water, and artificial seawater (Cai et al., 2018; Li et al., 2024; Su et al., 2024). However, such approaches may inadequately replicate natural marine dynamics, where synergistic physical abrasion (e.g., wave action) and microorganism (e.g., by *Marinobacter*, *Moraxella*, and *Rhodococcus*) accelerate surface degradation (Delacuvellerie et al., 2019; Gao et al., 2021; Li et al., 2024; Su et al., 2024). Furthermore, oceans act as long-term reservoirs for MPs, with hydrographic processes influencing their vertical transport and horizontal dispersion (Zhang et al., 2022). Therefore, it is imperative to investigate the aging process and mechanism of MPs in natural environments. Consequently, discrepancies likely exist between aging patterns observed in natural versus simulated seawater, necessarily investigating the aging process and mechanism of MPs in natural environments.

Despite advances in photodegradation research, critical knowledge gaps persist. First, few studies employ quantitative kinetic models (e.g., carbonyl index (CI)-based analyses) to systematically evaluate aging rates across MPs classes. Second, reliance on artificial media introduces uncertainties regarding real-world aging trajectories, particularly for heterogeneous marine environments. Are MPs degradation in real seawater consistent with the kinetic model observed in artificial seawater? We hypothesized that aging kinetics conform to degradation principles governed by MPs physicochemical properties.

Therefore, this study aims to investigate the influence of varying aging time on the degradation of MPs (i.e., mPE, mPP, mPS, and micro-sized polyvinyl chloride (mPVC)) in seawater under UVA irradiation by analyzing surface microstructure, elemental composition, crystallinity, and functional groups. Meanwhile, the CI was used to fit the First-order improvement kinetic model and the Elovich kinetic model to describe the degradation rate of MPs. Moreover, the impact of UVA aging on the degradation mechanism of MPs was discussed, aiming to develop more effective strategies for managing plastic waste and reducing marine environmental pollution.

# 2 Materials and methods

## 2.1 Materials

Four types of MPs (mPE, mPP, mPS, and mPVC) were selected for based on their high abundance in nearshore waters surrounding Hainan Island, China (Gao et al., 2022b). MPs with three distinct particle sizes (i.e., approximately 13, 165, and 550 μm), representative of the 10 μm–1 mm range prevalent in marine environments, were mechanically generated by Shunjie Technology Co., Ltd. (Dongguan, China). Key properties of the MPs are summarized in Supplementary Table S1. Spectroscopic grade potassium bromide was obtained from Aladdin Biochemical Technology Co., Ltd., Shanghai, China. Natural seawater was collected from Haikou, Hainan Province, China (20°3′48″E, 110°24′54″N), filtered through a 0.22 μm filter membrane. The physicochemical properties and compositions of seawater were shown in Supplementary Table S2, and specific determination methods were detailed in Supporting Information Text S1. A UVA-340 nm lamp (Q-Lab Corporation, USA; 20 W output, peak wavelength: 340 nm) was employed to simulate solar ultraviolet radiation.

## 2.2 UVA-aging of MPs

Pristine MPs were sequentially rinsed with deionized water, air-dried, and mixed with natural seawater in glass culture dishes (MPs: 3.5 g, seawater: 40 mL). Subsequently, all culture dishes were transferred to a custom-designed aging chamber (dimensions: 90 × 180 × 40 cm; Supplementary Figures S1a, b) maintained at 25°C for 15, 30, 90, and 180 days, with triplicate samples per timepoint. UVA possesses strong penetration capabilities, enabling it to traverse glass. Each chamber layer contained two UVA-340 tubes, delivering irradiance comparable to midday summer sunlight (0.70–0.80 μW/cm²) (Brennan, 1987). The UVA intensity was verified using a calibrated photometer (Sanpo Instrument Co., Ltd., China), measuring 78.1 μW/cm² at the lamp surface and 68.8 μW/cm² through the seawater-covered culture dish. To minimize evaporation, dishes were sealed with lids, and deionized water was replenished periodically (Supplementary Figure S1c). Post-aging, MPs were collected, surface-cleaned with deionized water, air-dried at room temperature, and stored in brown glass bottles for subsequent analysis (see Supporting Information 1 Text S2 for collection protocols).

## 2.3 Characteristics of MPs

The size of MPs was determined with a laser diffraction particle size analyzer (MAZ3000, Mastersizer, UK). The surface structures of MPs were examined by using Field Emission Scanning Electron Microscopy (FESEM, Verios G4 UC, Thermo Fisher Scientific, USA). The elemental composition of MPs surfaces was analyzed by using an X-ray Fluorescence Spectrometer (XRF, ArL Perform x, Thermo Scientific, USA). A Fourier Transform Infrared Spectrometer (FTIR, Tensor 27, Bruker, Germany) was employed to analyze the functional groups of MPs. An X-ray Diffractometer Spectrometer (XRD, DX-2700BH, Tianrui, China) was used to analyze the crystallinity of MPs. Triplicate measurements ensured reproducibility, with representative spectra selected for analysis. Details were provided in Supporting Information 1 Text 3.

## 2.4 MPs aging index

The CI is employed to quantitatively assess the degree of aging and oxidation in polymers, which is determined through analysis of FTIR spectra (Dong et al., 2022; Su et al., 2024). The CI calculation method was shown in Table 1. Initial attempts to model CI using a first-order kinetic equation yielded poor fits (Supplementary Table S3). Consequently, a modified first-order model incorporating an empirical parameter A and the Elovich kinetic model were applied to fit the CI (Table 1).

## 2.5 Data analysis

One-way analysis of variance (ANOVA) was performed using IBM SPSS 25 for statistical analysis, with significant differences assessed using the LSD multiple range test ($P$ <0.05). The FESEM images were annotated and combined using Adobe Photoshop 2021. The FTIR and crystallinity spectra were examined using the Thermo Scientific OMNIC Series and MDI Jade 6.5 software, respectively. Experimental data, CI fitting, and data visualization were conducted using Excel 2019 and Origin 2018.

TABLE 1 Calculation and fitting formula for the Carbonyl index (CI).

| Name/ model | Formula | Parameter |
|---|---|---|
| Carbonyl index | $CI = A_{1870-1650}/A_{1480-1440}$ | $A_{1480-1440}$ and $A_{1870-1650}$ are the FTIR characteristic peak area of methylene and carbonyl, respectively; $CI_a$ is $CI$ of pristine MPs; $T$ is MPs aging time (day); $CI_{rate}$ is an aging rate of $CI$ (day$^{-1}$); $CI_0$ is rate constant of $CI$ (day$^{-1}$); $K$ is first-order MPs aging rate constant; $A$ lacks practical significance; $a$ is the initial rate of aging; $b$ is the degradation ability during aging. |
| Carbonyl index rate | $CI_{rate} = (CI - CI_a)/T$ | |
| First-order kinetic | $CI = CI_0 e^{-KT}$ | |
| First-order kinetic improvement | $CI = CI_0 e^{-KT} + A$ | |
| Elovich kinetic | $CI = a + bln^T$ | |

# 3 Results and discussion

## 3.1 Surface structures of MPs

The aging process induced distinct structural alterations across MP types under UVA irradiation (Figure 1). While mPE, mPP, and mPS exhibited no significant color changes, mPVC developed a pronounced yellow hue after 180 days of exposure, indicative of surface oxidation and chromophore formation via photoinduced reactions (Sun et al., 2020). Plastic aging typically occurs through cracking and peeling. Initial surface analysis revealed smooth textures for pristine MPs (550 μm). However, progressive aging introduced structural defects, including flakes, cracks, protrusions, and oxidized particles (Figure 1), likely due to UVA radiation (Liu et al., 2020; Mao et al., 2020). Notably, the extent of deterioration varied with material and duration. For example, after 15-day aging, mPE and mPP developed noticeable particles, fragments, and cracks, while mPS showed minor fragmentation and mPVC remained mostly smooth with only a few fragments. After 30 days of aging, the aforementioned aging phenomenon became more pronounced. With prolonged aging time, the surfaces of MPs gradually transitioned from an initial smooth to rough. After 180-days aging, mPE and mPP exhibited disordered surface structures characterized by prominent pits, deep holes, and fractures; whereas mPS and mPVC displayed multiple cracks, numerous fragments, and particles.

Specifically, mPE contains unsaturated bonds (C=C) within the main chain or end chains, and exhibits frequent active branching points. These points are susceptible to oxidation by $O_3$, $NO_x$, or atmospheric free radicals, forming highly unstable hydrogen peroxide that subsequently transforms into stable carbonyl groups

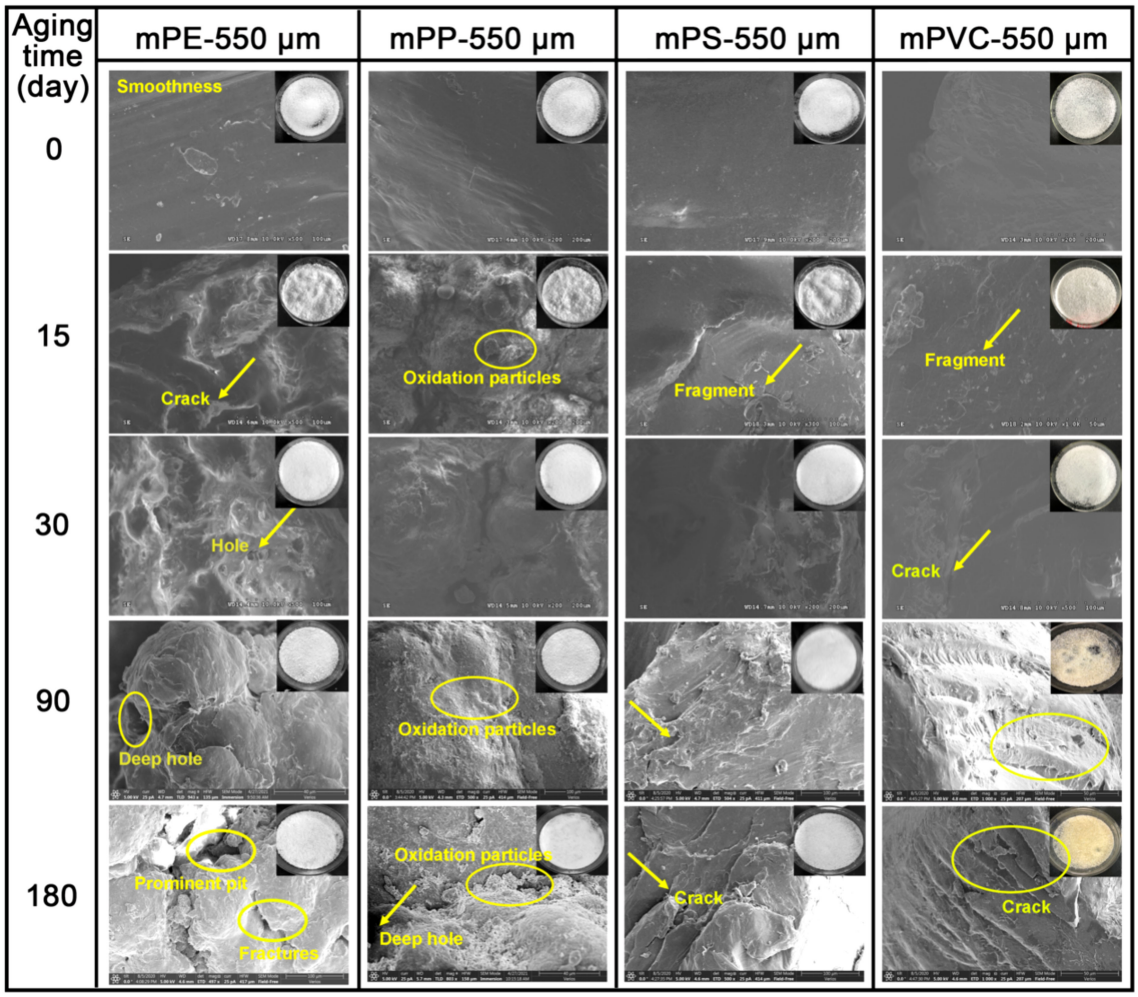


FIGURE 1
The FESEM and corresponding images of 550 μm MPs after aging for different days (0, 15, 30, 90 and 180 days).

with UVA absorption properties (Chamas et al., 2020; Rabek, 1995). mPP, especially in amorphous or low-order forms, is prone to oxidation at tertiary carbon atoms, leading to the formation and decomposition of hydrogen peroxides (Oswald and Turi, 1965). The migration of mPS free radicals within the polymer matrix induces degradation under UVA radiation, forming brittle regions or layers on their surface (Cooper, 2012; Yousif and Haddad, 2013). In contrast, mPVC's disordered open structure makes it less sensitive to UVA radiation and less susceptible to peeling (Arnold, 1995; Christensen et al., 2018). Furthermore, the accelerated aging in seawater compared to freshwater systems underscores the synergistic role of salinity. Chloride ions likely catalyzed hydrolysis and oxidative chain cleavage, enhancing surface roughness (Ding et al., 2020; Gao et al., 2021).

Moreover, some elements were detected on the surface of aged MPs, including Ag, Br, Ca, Cl, Fe, Ho, K, Lu, Mg, Si, Sr, Sx, Ti, Yb, and Zn (Figures 2a–d), indicating that MPs release internal structural elements during aging. The content of Ag, Br, Cl, Fe, K and Mg increased with prolonged aging time, suggesting progressive release of intrinsic additives (e.g., catalysts, plasticizers) from polymer matrices. For instance, Zn and Fe residues likely originated from Ziegler-Natta catalysts used in polyolefin synthesis (Groh et al., 2019; Turner and Filella, 2021). The emergence of surface cracks facilitated oxygen diffusion and elemental leaching, creating a feedback loop that accelerated oxidative degradation (Luo et al., 2020). Such elemental redistribution poses ecological risks, as heavy metals (e.g., Zn, Fe) may interact with marine biota or adsorb co-pollutants.

Comparative analysis of MPs across sizes (13 μm, 165 μm, 550 μm) revealed divergent aging trajectories (Supplementary Figure S2, S3). Larger MPs (550 μm) exhibited earlier onset of surface roughening (15 days vs. 30 days for 13 μm MPs). This may be attributed to higher surface-to-volume ratio in smaller particles, which delays crack initiation by distributing stress more evenly. Shorter diffusion pathways for oxygen and radicals in smaller MPs, promoting uniform oxidation over localized degradation (Liu et al.,

10.3389/fmars.2025.1519668

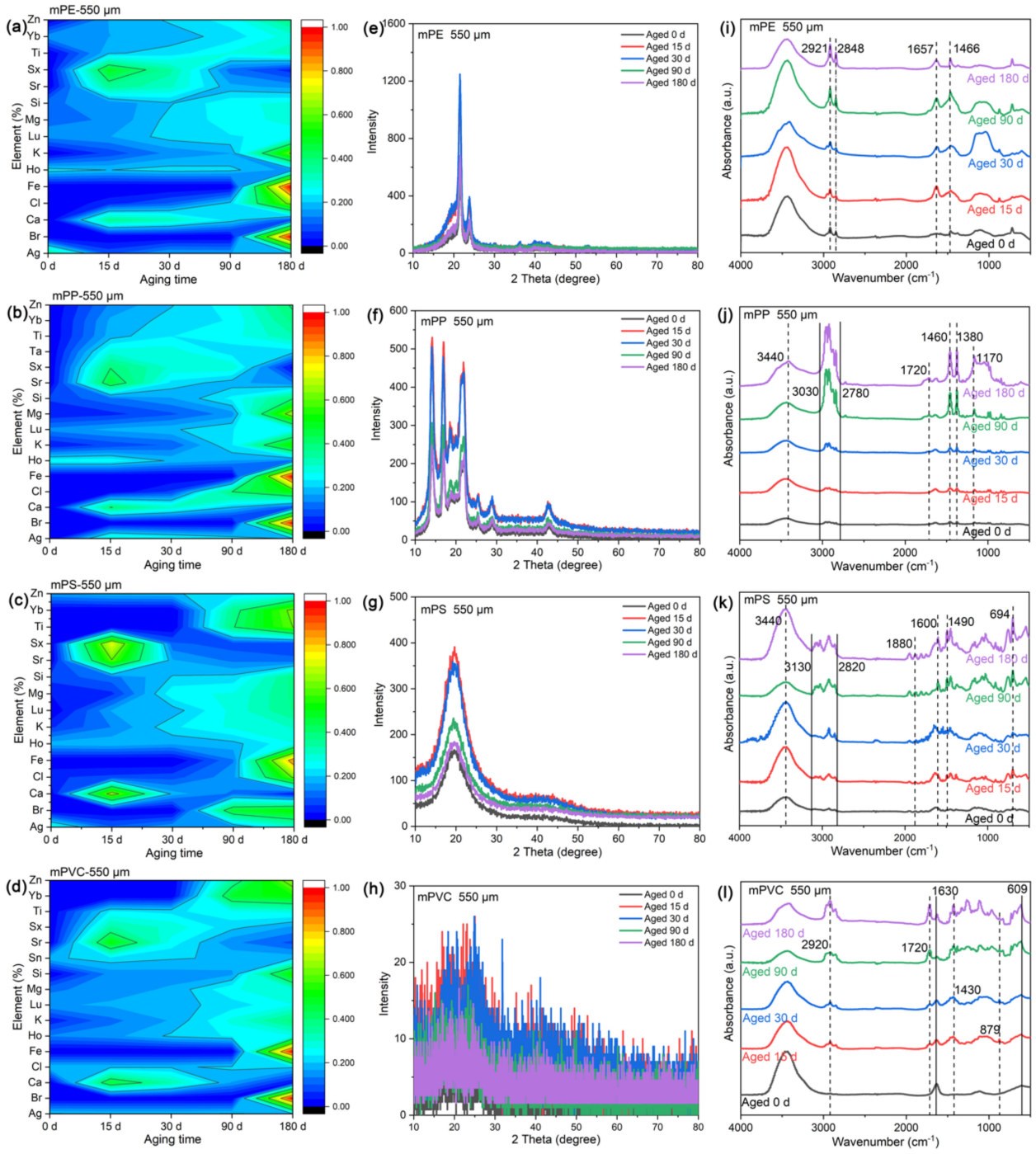


FIGURE 2
The surface characteristics (**(a-d)** surface element content, **(e-h)** crystallinity and **(i-l)** FTIR spectra) of 550 μm MPs after aging for different days; Notes: **(a, e, i)** mPE, **(b, f, j)** mPP, **(c, g, k)** mPS and **(d, h, l)** mPVC.

2020). Paradoxically, smaller MPs (13 μm) displayed higher surface elemental concentrations (Supplementary Figure S3), attributed to their greater specific surface area enhancing additive exposure and leaching (Mao et al., 2020). This inverse relationship between particle size and elemental release underscores the complexity of MPs aging mechanisms, necessitating multi-parameter assessments (e.g., CI, crystallinity) for holistic evaluation.

## 3.2 Crystallinity of MPs

XRD analysis revealed insights into the structural reorganization of MPs during UVA-induced aging. While mPVC exhibited complex diffraction patterns with overlapping peaks, precluding quantitative analysis, distinct crystallinity trends were observed for mPE, mPP, and mPS (Figures 2e–h).

No notable changes in the peak positions were observed in the four types of aged 550 µm MPs. mPE exhibited strong peaks at 21.5° and 23.9°, while mPP showed distinct peaks at 14.2°, 16.9°, and 21.9°. The primary peak for mPS was identified at 19.6°. Notably, the XRD spectra of aged MPs exhibited a noticeable increased peak intensity compared to pristine MPs. This suggests that aging affects MPs crystallinity, which is consistent with previous studies (Liu et al., 2018; Ma et al., 2019; Su et al., 2024). Additionally, this study revealed an intriguing phenomenon whereby the crystallinity of MPs diminishes over time. The crystallinity of aged 15 d MPs peaked, while the crystallinity of aged 180 d MPs only marginally surpassed that of pristine MPs. This may be attributed to the preferential degradation of amorphous regions during early aging stages, which temporarily increases crystallinity (Rouillon et al., 2016; Sun et al., 2020). Velzeboer et al. (2014) noted that oxidative damage to molecular chains can hinder crystal formation, reducing crystallinity after aging. The decrease of crystallinity of MPs may affect the change of the mass of the crystal region. UV aging can cause molecular chain breakage, leading to lower molecular weight and reduced crystal mass (Zhang et al., 2025). Additionally, new defect areas such as micropores and cracks may form during aging, further degrading crystal quality (Anshari et al., 2025).

Prolonged aging of MPs leads to the oxidation of amorphous regions, generating oxygen-containing functional groups and diminishing crystallinity. This phenomenon is mostly caused by oxidative reactions during continuous degradation of plastics, leading to chain fragmentation and incorporation of diverse polar functional groups. In particular, carbonyl groups tend to be enriched in the amorphous regions of polymers (Anshari et al., 2025). These groups can disrupt the regularity of molecular long chains and induce their entanglement, forming amorphous regions within MPs (Litvinov et al., 2020; Singh and Sharma, 2008). For instance, polyethylene terephthalate (PET) exposed to air shows higher CI values from peresters or anhydrides, indicating significant degradation in amorphous regions (Matsumoto et al., 2023). Various functional groups introduce compositional and structural diversity, causing variable changes in MPs' crystallinity levels. Decreased crystallinity enhances material brittleness while reducing toughness, accelerating plastic fracture (Dong et al., 2022).

Smaller MPs (165 µm) exhibited enhanced crystallinity compared to larger counterparts (550 µm). For mPE and mPP, peak intensities doubled in 165 µm MPs (Supplementary Figures S4a, b), attributable to higher surface area accelerating amorphous phase oxidation (Ma et al., 2019). Notably, 13 µm mPS showed a progressive peak shift from 19.6° to 14.5° after 90 days (Supplementary Figures S4e-g), signaling nanoscale structural reorganization via chain fragmentation. Though excluded from quantitative analysis, mPVC exhibited unique behavior: maximal diffraction intensity at 15 days (Supplementary Figures S4d, h), followed by progressive broadening. This suggests rapid additive leaching (e.g., plasticizers) initially stabilizes the structure, followed by chlorine loss-induced amorphization (Christensen et al., 2018). Overall, UVA radiation exposure increases MPs crystallinity and alters surface structure.

## 3.3 Functional groups of MPs

The interaction and cross-linking of free radicals in MPs can occur under UVA radiation, leading to external forces that impede segmental motion. This reduces elongation at break and increases brittleness (Galloway and Lewis, 2016; Liu et al., 2020). Besides surface morphology changes, the composition, properties, and functionalities of MP surfaces also modify during aging.

As shown in Figures 2i–l, FTIR spectra of pristine and aged MPs are similar. However, subtle changes and new peaks were observed in the functional groups corresponding to aged MPs, indicating modifications in the surface chemical structure of aged MPs. For instance, aged mPE displayed peaks at 2921, 2848, 1657, and 1466 $cm^{-1}$; aged mPP showed peaks at 3340, 3030-2780, 1720, 1460-1380, and 1170 $cm^{-1}$; aged mPS demonstrated peaks at 3440, 3130, 2820, 1880, 1600, 1490, and 694 $cm^{-1}$; whereas aged mPVC presented bands at wavelengths of 2920, 1720, and 1630–609 $cm^{-1}$ (e.g., 1430, 879 $cm^{-1}$). These deviations from pristine MPs suggest increased degradation with aging. Peak intensities of functional groups on MPs' surfaces become more prominent over time, especially after 180 days, confirming the detrimental impact of extended UVA radiation on the surface structure of MPs. This is consistent with previous studies showing that MPs undergo photooxidation under UVA exposure (Gao et al., 2022a).

The spectral range of 3750–3000 $cm^{-1}$ corresponded to hydroxyl (-OH) stretching vibration. The peak intensity of aged mPP and mPS was enhanced at 3440 $cm^{-1}$, indicating intensified -OH bonds stretching. Within the range of 3000–2700 $cm^{-1}$, novel peaks (mPP, mPS, mPVC) or stronger peak intensities (mPE) were observed, suggesting the presence of surface-bound C-H stretching (Table 2). UVA irradiation-induced degradation of MPs increases oxygen exposure, leading to extensive oxidation reactions (Cai et al., 2018; Yu et al., 2023). Moreover, the higher concentration of chloride ions in seawater facilitates substitution reactions, enhancing -OH stretching (Mao et al., 2020). The FTIR spectra of aged mPE, mPP, mPS, and mPVC exhibited significant changes in the carbonyl stretching vibration region (1900–1650 $cm^{-1}$), indicating C=O stretching (Table 2). Previous study showed that -OH and C=O serve as prominent indicators of polymer oxidation, with increased C=O implying the incorporation of oxygen into carbon-hydrogen bonds (Brandon et al., 2016). Additionally, aged samples also exhibited C=C double bond stretching in the 1690–1500 $cm^{-1}$. Within the 1475–1000 $cm^{-1}$ range, MPs displayed X-H in-plane bending vibrations, X-Y stretching vibrations, C-H in-plane bending or C-O stretching and skeletal vibrations associated with C-C single bonds (Table 2). The phenomenon may be attributed to the adsorption of substances, such as Laurocapram (aliphatic) and Phthalic anhydride (aromatic), by MPs in seawater (Supplementary Table S2). Previous studies demonstrated that MPs surfaces were rich in bisphenol A, polychlorinated biphenyls, nonylphenols, and other organic substances (Hirai et al., 2011; Mato et al., 2001; Pascall et al., 2005). Some research also indicated that mPE and micro-poly (butyleneadipate-co-terephthalate) (mPBAT) exhibited varying degrees of changes in aromatic and aliphatic C-O and C=O bonds under $H_2O_2$ influence (Du et al.,

TABLE 2 Typical functional groups of aged MPs in the aging band.

| Band name and range | Functional groups | Aging time (day) | | | |
|---|---|---|---|---|---|
| | | 15 | 30 | 90 | 180 |
| Hydroxyl stretching vibration region (3750–3000 $cm^{-1}$) | –OH stretching | ○□ | ○□ | ○ | ○□ |
| C–H stretching vibration region (3000–2700 $cm^{-1}$) | C–H stretching | •○□△ | •○□△ | •○□△ | •○□△ |
| Carbonyl stretching vibration region (1900–1650 $cm^{-1}$) | C=O stretching | ○□△ | ○□△ | ○□△ | ○□△ |
| Double bond stretching vibration region (1690–1500 $cm^{-1}$) | C=C stretching | •○□△ | •○□△ | •○□△ | •○□△ |
| X–H in-plane bending and X-Y stretching vibration region (1475-1000$cm^{-1}$) | C-H in-plane bending, C-O stretching | •○□△ | •○□△ | •○□△ | •○□△ |
| C-H out-of-plane bending vibration region (1000–650 $cm^{-1}$) | C-H out-of-plane bending | □ | □ | ○□△ | ○□△ |

The symbol "•" represents mPE; "○" represents mPP; "□" represents mPS; and "△" represents mPVC. These symbols indicate the functional groups detected in the corresponding spectral regions of aged MPs.

2024). MPs aging modifies surface morphology and functional groups, primarily due to fractured surfaces facilitating oxygen ingress and accelerating aging (Luo et al., 2020). After a 15-day aging period, novel peaks emerge within the range of 1000–650 $cm^{-1}$ for aged mPS; whereas for aged mPP and mPVC, new peaks begin to manifest after 90 days of aging, predominantly associated with out-of-plane bending vibrations of olefins and aromatics such as ortho-disubstituted benzene rings (770–735 $cm^{-1}$), meta-disubstituted benzene rings (710–690 and 810–750 $cm^{-1}$), and para-disubstituted benzene rings (830–810 $cm^{-1}$).

FTIR spectroscopy of MPs with smaller particle sizes (165 and 13 μm) showed that as aging time increased, differences in their infrared spectra became more pronounced. Aged MPs exhibited significant changes in C-H stretching vibrations (3000–2700 $cm^{-1}$), while aged mPS and mPVC showed more pronounced variations in out-of-plane bending vibrations (1000–650 $cm^{-1}$). In seawater conditions, long-wave ultraviolet irradiation affects MPs-oxygen interaction, leading to polymer chain breakage and crosslinking.

Meanwhile, FTIR spectroscopy of MPs with smaller particle sizes (i.e., 165 and 13 μm) revealed that as aging time increased, differences in their infrared spectra became more pronounced (Supplementary Figure S5). All aged MPs exhibited significant changes in functional groups within the C-H stretching vibration region (3000–2700 $cm^{-1}$), while aged mPS and mPVC showed more pronounced variations in the out-of-plane bending vibration region (1000–650 $cm^{-1}$). In conclusion, during photodegradation under seawater conditions, long-wave ultraviolet irradiation can affect MPs-oxygen interaction, leading to a cascade of physicochemical reactions such as polymer chain breakage and crosslinking.

## 3.4 MPs aging index

The CI serves as a reliable indicator of MPs aging, quantifying changes in carbonyl content and facilitating the evaluation of polymer chain breakage (Di Pippo et al., 2020). As shown in Figures 3a–d, the CI of aged MPs increased significantly over time: 180 d >90 d >30 d >15 d >0 d. Significant variations were observed before each treatment ($P$ <0.05), except for mPE-550 μm, mPE-165 μm, and mPP-550 μm. This result was consistent with previous research and can be primarily attributed to oxidation reactions on the surface of MPs under UVA irradiation (Dong et al., 2022; Zhang et al., 2023). The 550 μm mPE exhibited a higher CI value than the other two sizes of mPE (i.e., 165 and13 μm), likely due to its initially higher CI. The mPE and mPS exhibited higher CI values followed by mPVC, while mPP had the lowest. This indicated that different types of MPs exhibited varying degradation rates.

Simultaneously, the CI rate was calculated to quantify the aging rate of MPs. The mPE exhibited a significantly higher rate at 30 days of aging compared to other aging time ($P$ <0.05), ranging from 0.0200-0.0457% per day (Supplementary Table S4). A similar trend was observed for mPVC, while mPP and mPS demonstrated peak CI rates at 15 or 30 days of aging. The result is interpreted as substantial oxidation during the early stages of MP aging, consistent with previous findings on direct photolysis in early weathering (Dong et al., 2022). Moreover, smaller-sized MPs (i.e., 165 and 13 μm mPS, and 13 μm mPVC) exhibited lower CI rates, indicating slower degradation rate for small-sized MPs in the environment. The result was consistent with FESEM observations (Section 3.1). Therefore, more attention and concern should be paid to the small-sized MPs, particularly their potential environmental impact.

To gain a more profound insight into the aging process of MPs, this study aimed to correlate CI with aging time. Initially, a first-order kinetic model was employed to fit CI values; however, these fitting results were deemed unsatisfactory (Supplementary Table S3). Previous study also indicated that standard kinetic models were inadequate in explaining the degree of MPs aging or fragmentation (Di Pippo et al., 2020). While suitable for simple degradation processes, the first-order model is limited in complex scenarios with nonlinear behaviors and specific environmental conditions (Bekins et al., 1998; Wang et al., 2018). For example, factors such as temperature, pH levels, salinity, and microorganisms can influence reaction rates, leading to deviations from first-order kinetics. Although this study was conducted under UVA-340 irradiation and constant temperature, the presence of microorganisms in seawater complicates the degradation of MPs, thereby reducing the effectiveness of the first-order model.

To improve fitting accuracy, we incorporated an additional parameter into our modified first-order kinetic model. The fitting results demonstrated high accuracy (Figures 3e–h), with $R^2$ ranging

10.3389/fmars.2025.1519668

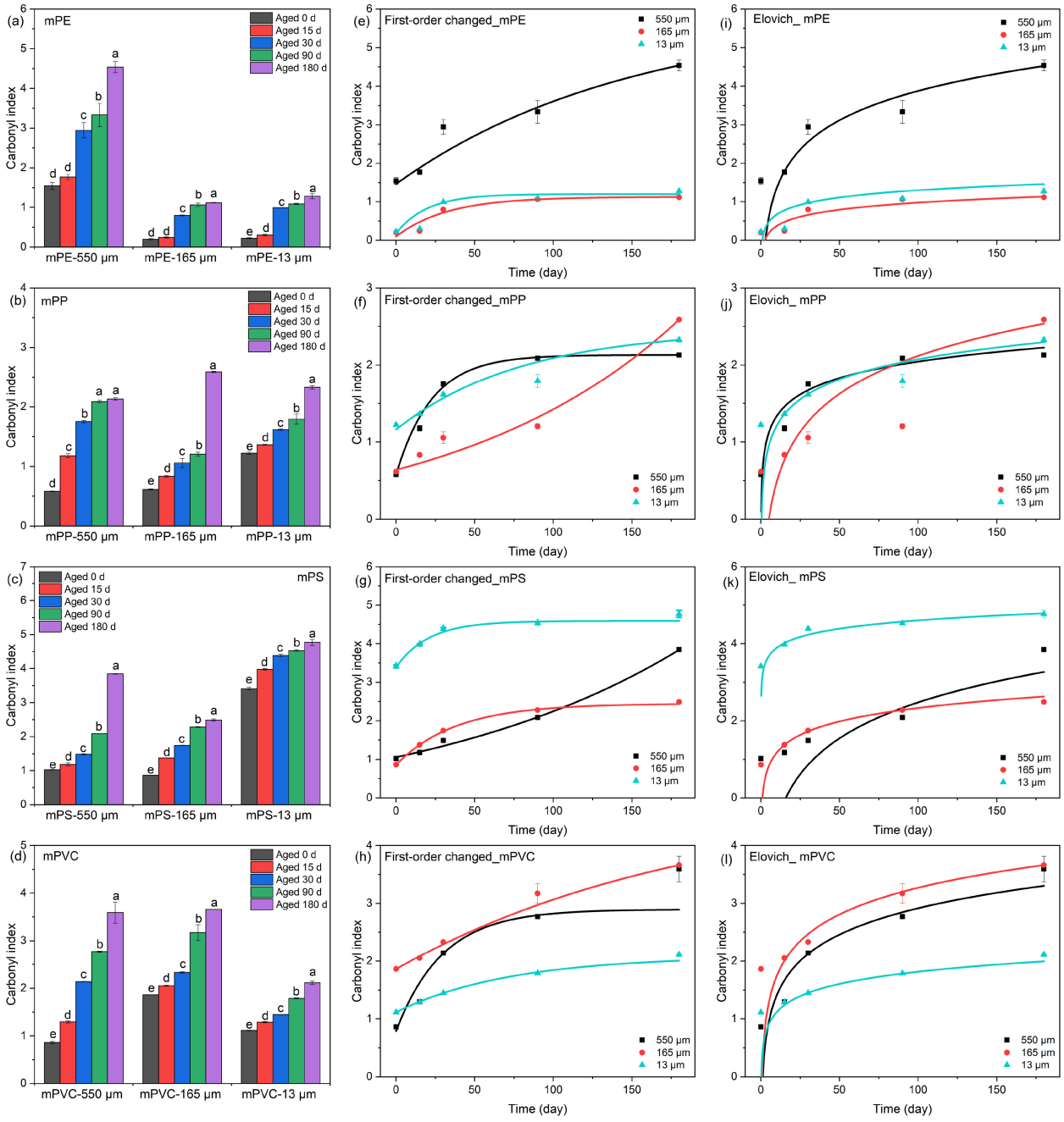


FIGURE 3
The **(a-d)** Carbonyl index of aged MPs, and kinetic models fitting **(e-h)** first-order kinetic improvement model, and **(i-l)** Elovich kinetic model.

from 0.88 to 0.99 (Supplementary Table S5). In contrast, previous study reported significantly lower $R^2$ of 0.774, 0.849, and 0.891 when employing first-order kinetics to fit mPP, mPET, and mPLA, respectively (Su et al., 2024), which contrasted sharply with our improved model in this study. However, further validation is necessary to confirm the significance of the parameters utilized in first-order kinetic improvement model. The Elovich model performed noticeably worse than our modified first-order model but showed satisfactory fits for 165 and 13 μm mPE, 165 μm mPP, as well as 550 μm mPVC, with $R^2$ ranging from 0.73 to 0.89. However, it performed poorly for mPS, with a maximum $R^2$ of 0.57 (Figures 3i–l and Supplementary Table S5). This highlights the complexity of MPs degradation in marine environments under UVA irradiation and underscores the limitations of simple kinetic models. This may be attributed to the material characteristics of MPs, including molecular weight, structure, and additives distribution significantly influence MPs degradation mechanism (Di Pippo et al., 2020; Liu et al., 2022).

In summary, the aging behavior of MPs is a complex environmental phenomenon requiring consideration of multiple

factors for thorough investigation. These factors encompass elements such as temperature, UV radiation, coexisting pollutants, and inherent material properties. Consequently, exploring the aging behavior of MPs remains a formidable challenge.

## 3.5 Mechanism of MPs degradation

The main chains of mPE, mPP, mPS, and mPVC are composed of carbon atoms, leading to similar photodegradation mechanisms in seawater. This process can be categorized into four steps: light initiation, free radical reaction, chain scission and surface oxidation (Figure 4). UVA irradiation cleaves C-H bonds, generating alkyl radicals (R•) that react with dissolved oxygen to form peroxyl radicals (ROO•) (Dimassi et al., 2022). These reactive intermediates abstract hydrogen from adjacent polymer chains, propagating radical chains and forming hydroperoxides (ROOH) (Ashfaq et al., 2020). Hydroperoxide photolysis (ROOH→RO• + •OH) induces backbone cleavage, reducing molecular weight and generating low-molecular-weight fragments (LMWFs) (Bracco et al., 2018). Concurrently, radical recombination promotes crosslinking, forming brittle three-dimensional networks (Gryn'ova et al., 2011). Oxidative functionalization introduces hydroxyl, carbonyl, and carboxyl groups (Figures 2i–l), enhancing hydrophilicity and microbial colonization (Gao et al., 2021; Gewert et al., 2015). FTIR spectra confirmed progressive CI increases, with mPE and mPP showing the highest oxidation levels after 180 days (Supplementary Table S4).

The degradation process of mPE in seawater is relatively straightforward. mPE degradation initiates via C-H bond cleavage at branching points, forming allylic radicals that rapidly oxidize to peroxides (Figure 4). This mechanism represents the crucial initial step in photodegradation (Bracco et al., 2018; Zhu et al., 2024), which was supported by the FTIR spectrum (Figure 2i). Chain scission produces LMWFs (<1 kDa), including aldehydes and ketones, which are readily metabolized by marine microbes to $CO_2$ and $H_2O$ (Ghatge et al., 2020). Crosslinking dominates at later stages, creating surface microcracks that accelerate embrittlement.

The tertiary carbons in mPP's -$CH_3$ side chains are highly susceptible to radical attack, leading to faster peroxide formation than mPE (Oswald and Turi, 1965). This results in 22.2% higher CI values for mPP compared to mPE after 180 days (Supplementary Table S4). Degradation generates methyl ketones and carboxylic acids, which enhance bioaccessibility but also increase ecotoxicity due to additive leaching (Gewert et al., 2015). Both mPE and mPP exhibited surface roughening under ultraviolet radiation, but the specific manifestations of these two types of MPs differ (Figure 1). Therefore, when investigating the weathering or degradation of MPs, it is important to consider the distinct degradation characteristics among different types of MPs.

The primary distinction in the degradation mechanism between mPS and mPE lies in the benzene ring, which can stabilize free radicals, slowing down the degradation rate of mPS (Yousif and Haddad, 2013). Prolonged UV exposure forms phenylperoxyl radicals (PhOO•), which decompose into benzaldehyde and benzoic acid—substances with demonstrated allelopathic effects

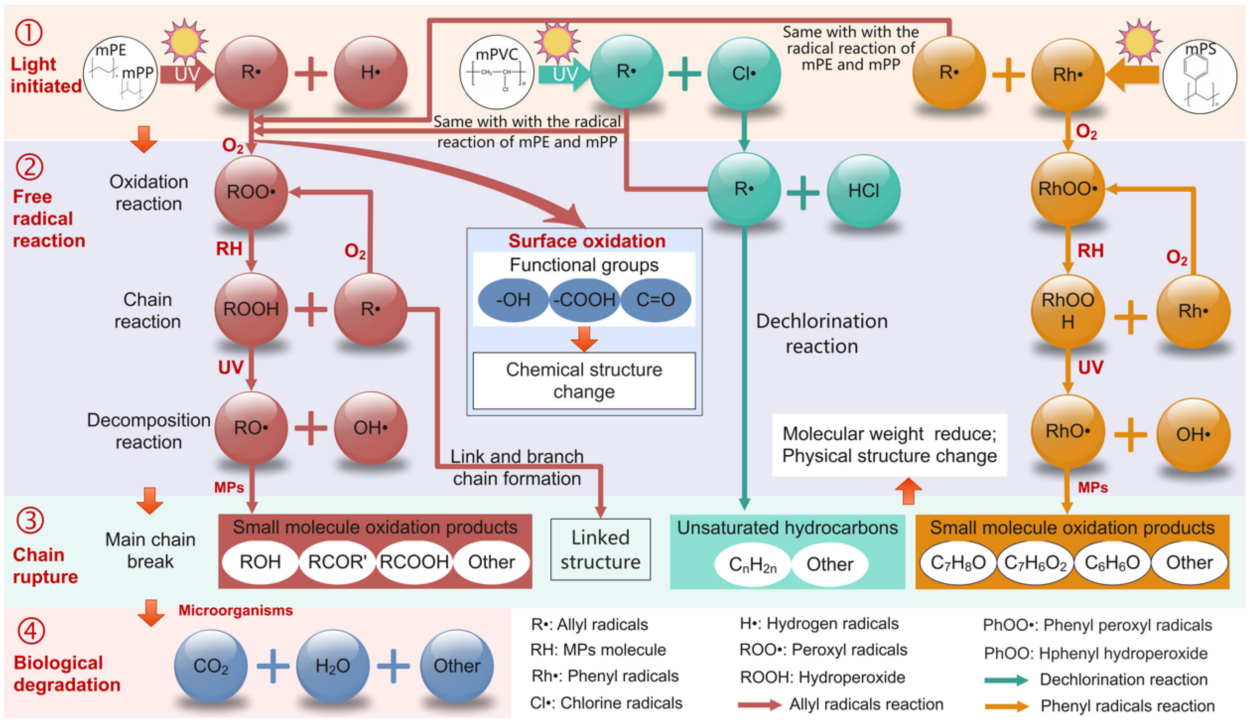


FIGURE 4
Degradation pathways of MPs.

on phytoplankton (Nakatani et al., 2022). FESEM images show that mPS has significantly lower surface roughness compared to mPE and mPP (Figure 1). Additionally, the CI for mPS was notably lower than that of mPE, especially after 180 days of aging. For instance, the CI for 13 μm mPE reached 0.0117 ± 0.0008, compared to 0.0076 ± 0.0007 for mPS (Supplementary Table S4).

The molecular structure of mPVC includes chlorine atoms, leading to a distinct photodegradation process in seawater compared to other MPs. mPVC undergoes dechlorination under UVA, cleaving C-Cl bonds to release HCl and chlorine radicals (Cl•) (Peng et al., 2022). The dechlorination process leads to a complex and slow degradation of mPVC (Kudzin et al., 2024), and the surface roughness of mPVC was significantly lower than other MPs (Figure 1). These radicals propagate chain scission, producing chlorinated LMWFs (e.g., dichloroethanes) that resist biodegradation and exhibit acute toxicity (Novotný et al., 2022). Surface Cl content increased by 18% after aging (Figures 2a, d, h), correlating with inhibited microbial activity in coastal sediments (Gao et al., 2023).

MPs degradation in seawater involves photodegradation and biodegradation, both influenced by environmental conditions such as salinity, temperature, and pH (Kaing et al., 2024). Elevated salinity and ionic diversity in seawater can affect MPs' surface properties, impacting pollutant adsorption and degradation. Lower seawater temperatures further inhibit both the rates of photodegradation and free radical reactions, but localized conditions (such as near hydrothermal vents or warm currents) can result in higher temperatures that may accelerate thermal degradation of MPs. pH influences the stability of oxidation products and microbial activity. In marine environments, physical processes such as wave action and sediment interactions cause mechanical abrasion of MPs (Sipe et al., 2022; Song et al., 2017). Additionally, microorganisms in marine environments can decompose MPs, but biodegradation is slow due to low oxygen levels and seawater temperatures. Meanwhile, MPs additives release substances during degradation, affecting the overall process (Gewert et al., 2015). The size and type of MPs also serve as influential factors on their degradation. In conclusion, the degradation rates of MPs can be ranked as follows: mPP >mPE >mPS >mPVC. A better understanding of these factors will aid in developing effective strategies for managing plastic waste and mitigating marine pollution.

## 4 Conclusion

In this study, the degradation rates of MPs can be ranked as follows: mPP >mPE > mPS >mPVC. The surface morphology and chemical properties of aged MPs were changed compared to pristine MPs, with the appearance of cracks, oxidized particles, wrinkles, changes in functional group stretching and crystallinity. After 180 days, aged MPs exhibited higher surface roughness and CI values. Variations in plastic composition contributed to differences in aging rates among the four types of MPs, with mPE and mPP showing the most pronounced aging effects. Although first-order kinetic improvement model exhibited better fitting performance between MPs' CI and aging time, the significance of its parameters remained uncertain. Therefore, simple kinetic models do not clearly capture the complexity of MPs aging that can be further explored. The degradation mechanisms of mPE and mPP are similar, while mPS involves benzene ring degradation and mPVC undergoes dechlorination. This study can further elucidate the aging properties and mechanisms of different MPs, thereby enhancing our understanding of the long-term weathering processes of MPs in marine environments and associated ecological risks.

## Data availability statement

The raw data supporting the conclusions of this article will be made available by the authors, without undue reservation.

## Author contributions

LG: Conceptualization, Software, Writing – original draft, Writing – review & editing, Data curation, Investigation, Methodology. YS: Methodology, Conceptualization, Project administration, Writing – original draft. TM: Conceptualization, Investigation, Writing – original draft. ZW: Investigation, Writing – original draft. LP: Conceptualization, Funding acquisition, Project administration, Supervision, Validation, Writing – review & editing. NZ: Funding acquisition, Investigation, Project administration, Writing – review & editing.

## Funding

The author(s) declare that financial support was received for the research and/or publication of this article. This study was supported, in part, by Yunnan Province Basic Research Program Youth Project (202501AU070035), Basic Research Project of Yunnan Provincial Department of Education (2025J0365), Hainan Natural Science Foundation Youth Fund Project (Excellent Youth Project, 424YXQN415), Key Project of Natural Science Foundation of Hainan Province, China (ZDYF2022SHFZ278), Hainan Talent Cultivation Project of the South China Sea - South China Sea Innovative Talent (the third batch), Joint Funds of the National Natural Science Foundation of China (U2002210), Yunnan Science and Technology Talent Platform Project (202405AM340004), Hainan key R&D program (ZDYF2025SHFZ062).

## Conflict of interest

The authors declare that the research was conducted in the absence of any commercial or financial relationships that could be construed as a potential conflict of interest.

## Generative AI statement

The author(s) declare that no Generative AI was used in the creation of this manuscript.

## Publisher's note

All claims expressed in this article are solely those of the authors and do not necessarily represent those of their affiliated organizations, or those of the publisher, the editors and the reviewers. Any product that may be evaluated in this article, or claim that may be made by its manufacturer, is not guaranteed or endorsed by the publisher.

## Supplementary material

The Supplementary Material for this article can be found online at: https://www.frontiersin.org/articles/10.3389/fmars.2025.1519668/full#supplementary-material

## References


Anshari, R., Tsuboi, M., Sato, H., Tashiro, K., and Ozaki, Y. (2025). Raman and ATR-FTIR unmask crystallinity changes and carboxylate group and vinyl group accumulation in natural weathering polypropylene microplastics. *Sci. Rep.* 15, 2518. doi: 10.1038/s41598-025-85837-y

Arnold, J. C. (1995). The influence of liquid uptake on environmental stress cracking of glassy polymers. *Mater. Sci. Engineering: A* 197, 119–124. doi: 10.1016/0921-5093(94)09759-3

Ashfaq, A., Clochard, M.-C., Coqueret, X., Dispenza, C., Driscoll, M. S., Ulański, P., et al. (2020). Polymerization reactions and modifications of polymers by ionizing radiation. *Polymers* 12, 2877. doi: 10.3390/polym12122877

Bekins, B. A., Warren, E., and Godsy, E. M. (1998). A comparison of zero-oder, first-order, and monod biotransformation models. *Groundwater* 36, 261–268. doi: 10.1111/j.1745-6584.1998.tb01091.x

Bracco, P., Costa, L., Luda, M. P., and Billingham, N. (2018). A review of experimental studies of the role of free-radicals in polyethylene oxidation. *Polym. Degrad. Stab.* 155, 67–83. doi: 10.1016/j.polymdegradstab.2018.07.011

Brandon, J., Goldstein, M., and Ohman, M. D. (2016). Long-term aging and degradation of microplastic particles: Comparing in *situ* oceanic and experimental weathering patterns. *Mar. pollut. Bull.* 110, 299–308. doi: 10.1016/j.marpolbul.2016.06.048

Brennan, P. J. (1987). Improved UV light source enhances correlation in accelerated weathering. *Plastics Compounding* 10, 25–28.

Cai, L., Wang, J., Peng, J. P., Wu, Z. Q., and Tan, X. (2018). Observation of the degradation of three types of plastic pellets exposed to UV irradiation in three different environments. *Sci. Total Environ.* 628-629, 740–747. doi: 10.1016/j.scitotenv.2018.02.079

Chamas, A., Moon, H., Zheng, J. J., Qiu, Y., Tabassum, T., Jang, J. H., et al. (2020). Degradation rates of plastics in the environment. *ACS Sustain. Chem. Eng.* 8, 3494–3511. doi: 10.1021/acssuschemeng.9b06635

Christensen, M. L., Klausen, M. M., and Christensen, P. V. (2018). Test of precoat filtration technology for treatment of swimming pool water. *Water Sci. Technol.* 77, 748–758. doi: 10.2166/wst.2017.593

Cooper, D. A. (2012). *Effects of chemical and mechanical weathering processes on the degradation of plastic debris on marine beaches* (London, Canada: University of Western Ontario).

Delacuvellerie, A., Cyriaque, V., Gobert, S., Benali, S., and Wattiez, R. (2019). The plastisphere in marine ecosystem hosts potential specific microbial degraders including *Alcanivorax borkumensis* as a key player for the low-density polyethylene degradation. *J. Hazardous Mater.* 380, 120899. doi: 10.1016/j.jhazmat.2019.120899

Dimassi, S. N., Hahladakis, J. N., Yahia, M. N. D., Ahmad, M. I., Sayadi, S., and Al-Ghouti, M. A. (2022). Degradation-fragmentation of marine plastic waste and their environmental implications: A critical review. *Arabian J. Chem.* 15, 104262. doi: 10.1016/j.arabjc.2022.104262

Ding, L., Mao, R., Ma, S., Guo, X., and Zhu, L. (2020). High temperature depended on the ageing mechanism of microplastics under different environmental conditions and its effect on the distribution of organic pollutants. *Water Res.* 174, 115634. doi: 10.1016/j.watres.2020.115634

Di Pippo, F., Venezia, C., Sighicelli, M., Pietrelli, L., Di Vito, S., Nuglio, S., et al. (2020). Microplastic-associated biofilms in lentic Italian ecosystems. *Water Res.* 187, 116429. doi: 10.1016/j.watres.2020.116429

Dong, S. Y., Yan, X. X., Yue, Y. Y., Li, W., Luo, W. Y., Wang, Y. Q., et al. (2022). $H_2O_2$ concentration influenced the photoaging mechanism and kinetics of polystyrene microplastic under UV irradiation: Direct and indirect photolysis. *J. Clean Prod.* 380, 135046. doi: 10.1016/j.jclepro.2022.135046

Du, T., Qian, L., Shao, S., Xing, T., Li, T., and Wu, L. (2024). Comparison of sulfide-induced transformation of biodegradable and conventional microplastics: Mechanism and environmental fate. *Water Res.* 253, 121295. doi: 10.1016/j.watres.2024.121295

Fang, S., Yu, W., Li, C., Liu, Y., Qiu, J., and Kong, F. (2019). Adsorption behavior of three triazole fungicides on polystyrene microplastics. *Sci. Total Environ.* 691, 1119–1126. doi: 10.1016/j.scitotenv.2019.07.176

Fu, D., Zhang, Q., Fan, Z., Qi, H., Wang, Z., and Peng, L. (2019). Aged microplastics polyvinyl chloride interact with copper and cause oxidative stress towards microalgae *Chlorella vulgaris*. *Aquat. Toxicol.* 216, 105319. doi: 10.1016/j.aquatox.2019.105319

Galloway, T. S., and Lewis, C. N. (2016). Marine microplastics spell big problems for future generations. *Proc. Natl. Acad. Sci. U. S. A.* 113, 2331–2333. doi: 10.1073/pnas.1600715113

Gao, L., Fu, D., Zhao, J., Wu, W., Wang, Z., Su, Y., et al. (2021). Microplastics aged in various environmental media exhibited strong sorption to heavy metals in seawater. *Mar. pollut. Bull.* 169, 112480. doi: 10.1016/j.marpolbul.2021.112480

Gao, L., Su, Y., Mehmood, T., Bao, R., and Peng, L. (2023). Microplastics leachate may play a more important role than microplastics in inhibiting microalga *Chlorella vulgaris* growth at cellular and molecular levels. *Environ. pollut.* 328, 121643. doi: 10.1016/j.envpol.2023.121643

Gao, L., Su, Y., Yang, L., Li, J., Bao, R., and Peng, L. (2022a). Sorption behaviors of petroleum on micro-sized polyethylene aging for different time in seawater. *Sci. Total. Environ.* 808, 152070. doi: 10.1016/j.scitotenv.2021.152070

Gao, L., Wang, Z., Peng, X., Su, Y., Fu, P., Ge, C., et al. (2022b). Occurrence and spatial distribution of microplastics, and their correlation with petroleum in coastal waters of Hainan Island, China. *Environ. pollut.* 294, 118636. doi: 10.1016/j.envpol.2021.118636

Gewert, B., Plassmann, M. M., and MacLeod, M. (2015). Pathways for degradation of plastic polymers floating in the marine environment. *Environ. Sci.: Processes Impacts* 17, 1513–1521. doi: 10.1039/c5em00207a

Ghatge, S., Yang, Y., Ahn, J.-H., and Hur, H.-G. (2020). Biodegradation of polyethylene: a brief review. *Appl. Biol. Chem.* 63, 27. doi: 10.1186/s13765-020-00511-3

Groh, K. J., Backhaus, T., Carney-Almroth, B., Geueke, B., Inostroza, P. A., Lennquist, A., et al. (2019). Overview of known plastic packaging-associated chemicals and their hazards. *Sci. Total Environ.* 651, 3253–3268. doi: 10.1016/j.scitotenv.2018.10.015

Gryn'ova, G., Hodgson, J. L., and Coote, M. L. (2011). Revising the mechanism of polymer autooxidation. *Org. Biomol. Chem.* 9, 480–490. doi: 10.1039/C0OB00596G

Hirai, H., Takada, H., Ogata, Y., Yamashita, R., Mizukawa, K., Saha, M., et al. (2011). Organic micropollutants in marine plastics debris from the open ocean and remote and urban beaches. *Mar. pollut. Bull.* 62, 1683–1692. doi: 10.1016/j.marpolbul.2011.06.004

Kaing, V., Guo, Z., Sok, T., Kodikara, D., Breider, F., and Yoshimura, C. (2024). Photodegradation of biodegradable plastics in aquatic environments: Current understanding and challenges. *Sci. Total Environ.* 911, 168539. doi: 10.1016/j.scitotenv.2023.168539

Kudzin, M. H., Piwowarska, D., Festinger, N., and Chruściel, J. J. (2024). Risks associated with the presence of polyvinyl chloride in the environment and methods for its disposal and utilization. *Materials* 17, 173. doi: 10.3390/ma17010173

Lang, M., Yu, X., Liu, J., Xia, T., Wang, T., Jia, H., et al. (2020). Fenton aging significantly affects the heavy metal adsorption capacity of polystyrene microplastics. *Sci. Total Environ.* 722, 137762. doi: 10.1016/j.scitotenv.2020.137762

Li, Y., Xu, G., and Yu, Y. (2024). Freeze-thaw aged polyethylene and polypropylene microplastics alter enzyme activity and microbial community composition in soil. *J. Hazardous Mater.* 470, 134249. doi: 10.1016/j.jhazmat.2024.134249

Litvinov, V., Deblieck, R., Clair, C., Van den Fonteyne, W., Lallam, A., Kleppinger, R., et al. (2020). Molecular structure, phase composition, melting behavior, and chain entanglements in the amorphous phase of high-density polyethylenes. *Macromolecules* 53, 5418–5433. doi: 10.1021/acs.macromol.0c00956

Liu, J., Ma, Y., Zhu, D., Xia, T., Qi, Y., Yao, Y., et al. (2018). Polystyrene nanoplastics-enhanced contaminant transport: Role of irreversible adsorption in glassy polymeric domain. *Sci. Total Environ.* 52, 2677–2685. doi: 10.1021/acs.est.7b05211

Liu, L., Xu, M., Ye, Y., and Zhang, B. (2022). On the degradation of (micro)plastics: Degradation methods, influencing factors, environmental impacts. *Sci. Total Environ.* 806, 151312. doi: 10.1016/j.scitotenv.2021.151312

Liu, P., Zhan, X., Wu, X., Li, J., Wang, H., and Gao, S. (2020). Effect of weathering on environmental behavior of microplastics: Properties, sorption and potential risks. *Chemosphere* 242, 125193. doi: 10.1016/j.chemosphere.2019.125193

Luo, H., Zhao, Y., Li, Y., Xiang, Y., He, D., and Pan, X. (2020). Aging of microplastics affects their surface properties, thermal decomposition, additives leaching and interactions in simulated fluids. *Sci. Total Environ.* 714, 136862. doi: 10.1016/j.scitotenv.2020.136862

Ma, J., Zhao, J., Zhu, Z., Li, L., and Yu, F. (2019). Effect of microplastic size on the adsorption behavior and mechanism of triclosan on polyvinyl chloride. *Environ. pollut.* 254, 113104. doi: 10.1016/j.envpol.2019.113104

Mao, R., Lang, M., Yu, X., Wu, R., Yang, X., and Guo, X. (2020). Aging mechanism of microplastics with UV irradiation and its effects on the adsorption of heavy metals. *J. Hazardous Mater.* 393, 122515. doi: 10.1016/j.jhazmat.2020.122515

Mato, Y., Isobe, T., Takada, H., Kanehiro, H., Ohtake, C., and Kaminuma, T. (2001). Plastic resin pellets as a transport medium for toxic chemicals in the marine environment. *Environ. Sci. Technol.* 35, 318–324. doi: 10.1021/es0010498

Matsumoto, T., Yorifuji, M., Hori, R., Hara, M., Yamada, N. L., Seto, H., et al. (2023). Selective acetylation of amorphous region of poly(vinyl alcohol) in supercritical carbon dioxide. *Polym. J.* 55, 1287–1293. doi: 10.1038/s41428-023-00832-2

Nakatani, H., Ohshima, Y., Uchiyama, T., and Motokucho, S. (2022). Degradation and fragmentation behavior of polypropylene and polystyrene in water. *Sci. Rep.* 12, 18501. doi: 10.1038/s41598-022-23435-y

Novotný, Č., Fojtík, J., Mucha, M., and Malachová, K. (2022). Biodeterioration of compost-pretreated polyvinyl chloride films by microorganisms isolated from weathered plastics. *Front. Bioeng. Biotechnol.* 10. doi: 10.3389/fbioe.2022.832413

Oswald, H. J., and Turi, E. (1965). The deterioration of polypropylene by oxidative degradation. *Polymer Engineering & Science* 5 (3), 118–207. doi: 10.1002/pen.760050312

Pascall, M. A., Zabik, M. E., Zabik, M. J., and Hernandez, R. J. (2005). Uptake of polychlorinated biphenyls (PCBs) from an aqueous medium by polyethylene, polyvinyl chloride, and polystyrene films. *J. Agric. Food Chem.* 53, 164–169. doi: 10.1021/jf048978t

Peng, L., Fu, D., Qi, H., Lan, C., Yu, H., and Ge, C. (2020). Micro- and nano-plastics in marine environment: Source, distribution and threats - A review. *Sci. Total Environ.* 698, 134254. doi: 10.1016/j.scitotenv.2019.134254

Peng, T., Xu, C., Yang, L., Yang, B., Cai, W.-W., Gu, F., et al. (2022). Kinetics and mechanism of degradation of reactive radical-mediated rrobe compounds by the UV/chlorine process: Theoretical calculation and experimental verification. *ACS Omega* 7, 5053–5063. doi: 10.1021/acsomega.1c06001

Rabek, J. F. (1995). *Polymer Photodegradation: Mechanisms and Experimental Methods* (London: Chapman & Hall).

Rochman, C. M., Hoh, E., Hentschel, B. T., and Kaye, S. (2013). Long-term field measurement of sorption of organic contaminants to five types of plastic pellets: Implications for plastic marine debris. *Environ. Sci. Technol.* 47, 1646–1654. doi: 10.1021/es303700s

Rouillon, C., Bussiere, P. O., Desnoux, E., Collin, S., Vial, C., Therias, S., et al. (2016). Is carbonyl index a quantitative probe to monitor polypropylene photodegradation? *Polym. Degrad. Stab.* 128, 200–208. doi: 10.1016/j.polymdegradstab.2015.12.011

Singh, B., and Sharma, N. (2008). Mechanistic implications of plastic degradation. *Polym. Degrad. Stab.* 93, 561–584. doi: 10.1016/j.polymdegradstab.2007.11.008

Sintim, H. Y., Bary, A. I., Hayes, D. G., English, M. E., Schaeffer, S. M., Miles, C. A., et al. (2019). Release of micro- and nanoparticles from biodegradable plastic during in *situ* composting. *Sci. Total Environ.* 675, 686–693. doi: 10.1016/j.scitotenv.2019.04.179

Sipe, J. M., Bossa, N., Berger, W., von Windheim, N., Gall, K., and Wiesner, M. R. (2022). From bottle to microplastics: Can we estimate how our plastic products are breaking down? *Sci. Total Environ.* 814, 152460. doi: 10.1016/j.scitotenv.2021.152460

Song, Y. K., Hong, S. H., Jang, M., Han, G. M., Jung, S. W., and Shim, W. J. (2017). Combined effects of UV exposure duration and mechanical abrasion on microplastic fragmentation by polymer type. *Environ. Sci. Technol.* 51, 4368–4376. doi: 10.1021/acs.est.6b06155

Stark, N. M., and Matuana, L. M. (2004). Surface chemistry changes of weathered HDPE/wood-flour composites studied by XPS and FTIR spectroscopy. *Polym. Degrad. Stab.* 86, 1–9. doi: 10.1016/j.polymdegradstab.2003.11.002

Su, X., Liu, M., Dai, H. Y., Dou, J. B., Lu, Z. J., Xu, J. M., et al. (2024). Novel insight into the aging process of microplastics: An *in-situ* study in coastal wetlands. *Water Res.* 248, 120871. doi: 10.1016/j.watres.2023.120871

Sun, Y., Yuan, J., Zhou, T., Zhao, Y., Yu, F., and Ma, J. (2020). Laboratory simulation of microplastics weathering and its adsorption behaviors in an aqueous environment: A systematic review. *Environ. pollut.* 265, 114864. doi: 10.1016/j.envpol.2020.114864

Turner, A., and Filella, M. (2021). Hazardous metal additives in plastics and their environmental impacts. *Environ. Int.* 156, 106622. doi: 10.1016/j.envint.2021.106622

Velzeboer, I., Kwadijk, C. J. A. F., and Koelmans, A. A. (2014). Strong sorption of PCBs to nanoplastics, microplastics, carbon nanotubes, and fullerenes. *Environ. Sci. Technol.* 48, 4869–4876. doi: 10.1021/es405721v

Wang, Y., Qin, C., and Witarsa, F. (2018). Clarifying configurations of reaction rate constant for first-order and Monod-type kinetics: A comparative manner and a pursuit of parametric definition. *Waste Manage.* 77, 22–29. doi: 10.1016/j.wasman.2018.04.040

Yousif, E., and Haddad, R. (2013). Photodegradation and photostabilization of polymers, especially polystyrene: review. *Springerplus* 2, 398. doi: 10.1186/2193-1801-2-398

Yu, Y., Astner, A. F., Zahid, T. M., Chowdhury, I., Hayes, D. G., and Flury, M. (2023). Aggregation kinetics and stability of biodegradable nanoplastics in aquatic environments: Effects of UV-weathering and proteins. *Water Res.* 239, 120018. doi: 10.1016/j.watres.2023.120018

Zhang, M., Lin, Y., Booth, A. M., Song, X., Cui, Y., Xia, B., et al. (2022). Fate, source and mass budget of sedimentary microplastics in the Bohai Sea and the Yellow Sea. *Environ. pollut.* 294, 118640. doi: 10.1016/j.envpol.2021.118640

Zhang, Y., Liu, C., Chen, K., Fan, J., Zhang, Z., Li, B., et al. (2025). Comprehensive study of the steam-aging degradation behaviors and its correspondence to aging mechanism of PET monofilaments under artificially accelerated environment. *Polymer* 322, 128159. doi: 10.1016/j.polymer.2025.128159

Zhang, Z. A., Qin, X., and Zhang, Y. (2023). Using data-driven methods and aging information to quantitatively Identify microplastic environmental sources and establish a comprehensive discrimination index. *Environ. Sci. Technol.* 57, 11279–11288. doi: 10.1021/acs.est.3c03048

Zhu, Z., Cao, X., Wang, K., Guan, Y., Ma, Y., Li, Z., et al. (2024). The environmental effects of microplastics and microplastic derived dissolved organic matter in aquatic environments: A review. *Sci. Total Environ.* 933, 173163. doi: 10.1016/j.scitotenv.2024.173163